

PAPER • OPEN ACCESS

Qualification and test of space compatible superconducting current leads (REBCO) designed for adiabatic demagnetization refrigerators

To cite this article: J M Duval *et al* 2024 *IOP Conf. Ser.: Mater. Sci. Eng.* **1302** 012014

View the [article online](#) for updates and enhancements.

You may also like

- [The influence of harness parasitic parameters of arc power supply controllers](#)
Zheng Peng, Zongliang Li, Ze Li et al.
- [THE MANGA INTEGRAL FIELD UNIT FIBER FEED SYSTEM FOR THE SLOAN 2.5 M TELESCOPE](#)
N. Drory, N. MacDonald, M. A. Bershadly et al.
- [Thermodynamic machine learning through maximum work production](#)
Alexander B Boyd, James P Crutchfield and Mile Gu

Qualification and test of space compatible superconducting current leads (REBCO) designed for adiabatic demagnetization refrigerators

J M Duval¹, T Prouvé¹, M Collier-Wright², A Drechsler³, D Hindley², M La Rosa Betancourt², R Kroll⁴, M Branco⁴, D Orgaz Diaz⁵, S I Schlachter³

¹ Univ. Grenoble Alpes, CEA, IRIG, DSBT, F-38000 Grenoble, France

² Neutron Star Systems, Moltkestr. 127, 50674 Cologne, Germany

³ Karlsruhe Institute of Technology, Institute for Technical Physics, Hermann-von-Helmholtz-Platz 1, 76344 Eggenstein-Leopoldshafen, Germany

⁴ European Space Agency (ESA), ESTEC, Keplerlaan 1, PO Box 299, NL-2200 AG Noordwijk, The Netherlands

⁵ Madrid Space, Av. Gregorio Peces Barba, 1, 28919 Leganés, Madrid, Spain

Email: jean-marc.duval@cea.fr

Abstract. Many astrophysics observations require space telescopes, either to reduce atmospheric perturbation or simply to make these detections possible (in the X-Ray spectrum for example). One of these missions, Athena, is led by the European Space Agency (ESA), with additional international contributions, dedicated to X-Ray observation. Two instruments will be part of this mission and among them, X-IFU, will use Transition Edge Sensors (TES) to detect and precisely measure the energy of X-Ray photons. These sensors require a temperature of 50 mK to reach their ambitious sensitivity goals. In space, this temperature can be reached using Adiabatic Demagnetization Refrigeration (ADR) and such a cooling system is currently being developed for the X-IFU instrument. ADR utilizes magnetocaloric materials which, upon variation in magnetic fields, can produce a cooling effect. The magnetic field of the order of 1 T in a volume of 10s of cm³ is produced by a superconducting coil with high winding number and current limited to approximately 2 A. Even though this current is low compared to most earth-based systems, metallic current leads to link the high- and low-temperature stages would cause high thermal loads, unacceptable for the limited capacity of the cryogenic cooling chain of the spacecraft. Therefore, a harness consisting of superconducting current leads is planned to reduce the thermal loads at the low-temperature stage. As part of an ESA contract, our team designed, built and tested such a space-compatible harness. This harness includes the electrical interfaces at both ends as well as mechanical support. Its development is capable of operating between interfaces at 80 K and 4 K. The harness is based on industrially available Rare-Earth-Barium-Copper-Oxide (REBCO) High-Temperature Superconductor (HTS) tapes. The tapes were laser-cut by our group to fulfill our specifications, Parylene coated and reinforced with Kapton laminate tape for mechanical and insulating purposes. After characterization of the single tapes, the assembled harness has been subjected to an extensive qualification sequence including thermal cycling and mechanical testing based on launch loads requirements. This paper will summarize the technical design choices for this HTS harness. It will discuss the test results and propose some perspectives for the next iteration of the development.



1. Introduction

Very low temperature is a key for astrophysics to reach the most demanding sensitivity. At this date, three space observatories have operated with temperatures at or lower than 100 mK. Two used magnetic cooling as the refrigeration method: XRS-2 instrument on ASTRO-E2 (renamed Suzaku after launch) and SXS instrument on ASTRO-H (renamed HITOMI after launch). Dilution cooling were used on the Planck satellite to cool the detectors to 100 mK. Several new programs requiring temperatures of 50 to 100 mK are under study, including the instrument X-IFU (X-ray Integral Field Unit) of the Athena (Advanced Telescope for High ENergy Astrophysics) mission [1]. This is a mission led by the European Space Agency (ESA) dedicated to the study of the hot and energetic universe, which will conduct X-ray observation thanks to two instruments. The cooling planned for the X-IFU instrument is a 50 mK cooler built on adiabatic demagnetization refrigerators (ADR) technology.

Magnetic cooling, or ADR, are based on the change of temperature or heat of a material when subject to a change of magnetic field. This technology is very well adapted to space cooling, as it is insensitive to gravity. One of the most discussed drawbacks from space application is its weight, which is induced by the need for magnetic shielding. Another major point is the need for current leads to carry the current for the superconducting coil. As opposed to most ground-based operations, for space instruments, the thermal resources are extremely limited, including at the intermediate temperature stages. For example at 100 K or 50 K, typically the cooling is achieved either via passive cooling, such as V-groove radiators, or via space coolers. The order of magnitude of the cooling power is of only several watts.

1.1. How high are high currents?

For metallic non-superconducting optimized current leads the cooling power P required to compensate ohmic losses and losses due to heat conduction can be derived from the application of the Wiedemann-Franz law and is approximately equal to:

$$P = I \sqrt{L_0 (T_{warm}^2 - T_{cold}^2)}$$

where I is the current, T_{warm} and T_{cold} the temperatures of the warm and cold end, respectively, and L_0 is the Lorentz number, experimentally evaluated to be $2.44 \cdot 10^{-8} \text{ V}^2/\text{K}^2$.

This equation shows that, contrary to intuition, the power load of optimized current lead is independent of the material properties and of the length between each stage, assuming the diameter is optimized. It is worth noting that this equation should be considered an order of magnitude as several factors play a role. First, materials do not exactly follow the Wiedemann-Franz law and it is possible to benefit from small deviations. Secondly, for real use cases with varying currents, optimization could be achieved at a lower current than the design current, reducing the average dissipation.

This equation shows the proportionality between the current and the heat load on the interfaces. Considering the cooling power available from a space cooler such as pulse tube coolers is small compared to ground experiments : typically 450 mW at 15 K and a few watts at 100 K [2], it is clear that the current must be limited to acceptable values. The full optimization of the current is out of the scope of the discussion as it implies system studies of cryogenics chain performance and manufacturability and mass of ADR stages. As a standard value, the typical order of magnitude of current in space instruments with ADR magnets is 2 A.

1.2. The need for superconducting harnesses

Once again, applying the Wiedemann-Franz law for the last stage and comparing the values to typical cooling power of space coolers rapidly demonstrates the need for the use of superconducting current leads.

Considering a current lead comprising two conductors designed for a current of 2 A, a warm temperature of 30 K – or 15 K - , the estimated thermal load on a cold interface at 4 K is respectively 18.5 mW – or 9 mW. These numbers should be compared to about 30 mW from 4 K-class Joule-Thomson coolers [3] that should be used mainly for the thermo-mechanical design of the instrument as well as for the heat lift of subkelvin coolers. Superconducting current leads, with no joule heating and

greatly reduced heat conduction contributions, are therefore necessary for the coldest stage of the harness.

1.3. State of the art

Several current lead harness technologies have been developed in the past, using MgB_2 wires [4] or HTS tapes [5]. MgB_2 offers advantages in terms of integration, handling, and heat conductivity. Its transition temperature, however, is 39 K, which restricts its use to temperatures below 30 K to include margins. This is not sufficient for the considered design, consequently our work focused on using HTS REBCO tapes, which can achieve transition temperatures above 90 K. REBCO tapes moreover have the advantage of a higher industrial maturity and are commercially available. Generally, CFRP has been used as mechanical support for past developments.

2. Design

Our design process has been described in [6] in detail and is summarized here. The first step of the design is the choice of REBCO tape. After an extensive study, two industrially available tapes have been considered, differing mostly in their critical temperature and their cap layer: one from Superpower with AgAu5% caplayer, and the other one from SuperOx with Ag cap layer. Both tapes are based on a Hastelloy substrate. The Hastelloy thickness differs as depicted in Table 1, but in any case, its contribution to the total heat conductivity is very limited. The difference in the cap layer, however, has a direct impact on the heat conductivity as presented in figure 1. For availability reasons, as well as to follow a strict requirement to ensure warm end operation at 85 K, in this first step of the development the Ag-coated wire with higher T_c has been used. In future phases of the development with more drastic constraints on heat conductivity, especially for multi-stage ADRs, the use of AgAu-coated tapes will be reconsidered due its superior thermal properties.

Table 1. Main design properties of the two selected tapes

	Superpower	SuperOx
Substrate	50 μm Hastelloy	43 μm Hastelloy
Cap layer	AgAu5%	Ag 2.5 μm + 1.3 μm
Critical current	93 K	89 K

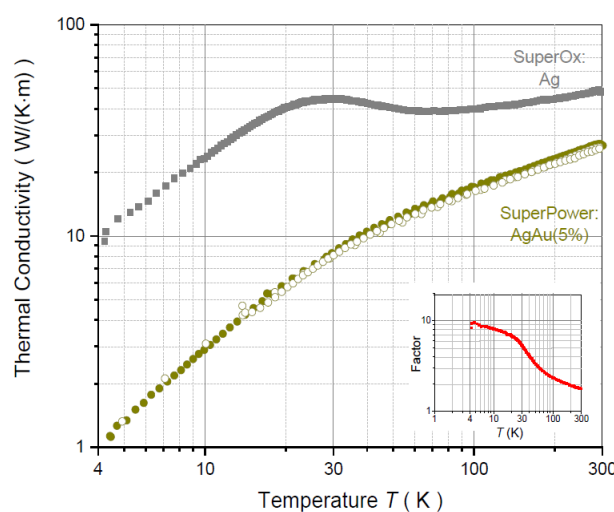


Figure 1. Heat conductivity based on KIT measurements (from [6]). The subset chart present the ratio SuperOx/Superpower thermal conductivity (“factor”).

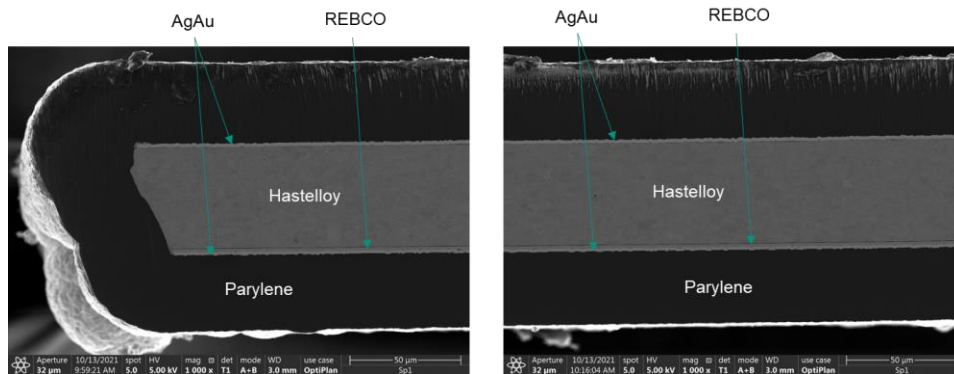


Figure 2. Parylene coating of the RebcO wire

For industrial reasons, HTS tapes are usually manufactured in a width of 12 mm. This width gives access to critical current of several 100 A, much higher than our requirement. The adverse impact is that the large cross-section leads to higher heat conductivity, too high for our specification. The first step of manufacturing is therefore laser-cutting. This step reduces the width of each tape to 1 mm. Because of the laser cutting, and in any case for long lifetime requirements for space use, including storage and testing phase before launch, a strong protection against humidity is required. To this end, a layer of Parylene coating on the tape is applied as a first layer of protection. A SEM (Scanning Electron Microscope) picture of a SuperPower tape – not selected finally – after Parylene coating is presented in figure 2. Finally, for mechanical reasons Kapton tape is laminated directly to the assembly. This Kapton tape is crucial for the assembly to withstand the mechanical loads applied to simulate the launch conditions.

The next step of the design is the integration of this laminated tape into a full harness. Connectors at the warm and cold interfaces are added as well as intermediate thermal and mechanical supports. As required by ESA, the length between each interface is 250 mm. This is longer than typical applications and because of the moment of inertia of a parallelepiped proportional to the cube of the length, reducing this length would drastically reduce the mechanical constraints during launch or qualification.

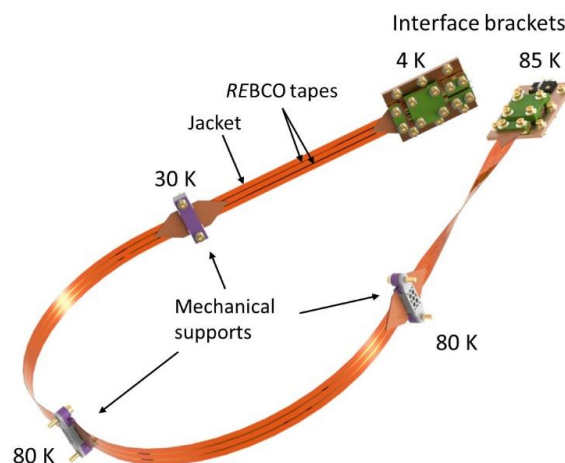


Figure 3. CAD Drawing of the full assembly of the HTS Harness including connectors and thermal/mechanical interface

The final design, shown in figure 3, can include bends and twists. Two models have been manufactured and characterized. The first model has been used to debug and improve the thermal and electrical test set-up. The second model underwent the full characterization and qualification sequence. The measurements are presented only for the second harness.

3. Performance characterization

Prior to the final manufacturing, mechanical tests on a short sample have been conducted. These tests showed no degradation after representative mechanical constraints similar to the test campaign (see further in the article) and it was decided to go ahead with this design. After manufacturing of the full 1-meter harness, the main performances of the harness have been verified. The verification included the nominal operation of the HTS harness with the nominal current of 2 A and even up to 5 A for full validation. In addition, it includes the experimental evaluation of heat flow on the various interfaces in different conditions.

3.1. Measurement setup

For the characterization, a dedicated thermal test bench has been designed and integrated into a helium cryostat. It is based on a 4.2 K plate. Thermally insulating supports are used for each interface. Each support includes a calibrated thermal link, a heater and a thermometer making heat flow measurements possible. This setup, as well as the interfaces, are schematized in figure 4. The temperature is regulated at the interface and the variation of the power when conditions (such as temperature of another interface) are changing. This principle makes precise measurements down to 10 or 100 μ W possible. The post G and F are necessary in addition to the supports to be able to apply a well-defined additional load – simulating the heat load from the metallic harness on E. This setup makes precise measurements feasible in a very flexible way, but is limited to eliminate the impact of radiation. Having 80 K parts within a 4 K cryostat makes measurements more complicated. The proposed way to deal with this limitation is to separate all measurements and evaluate the contribution of all parameters one after the other.

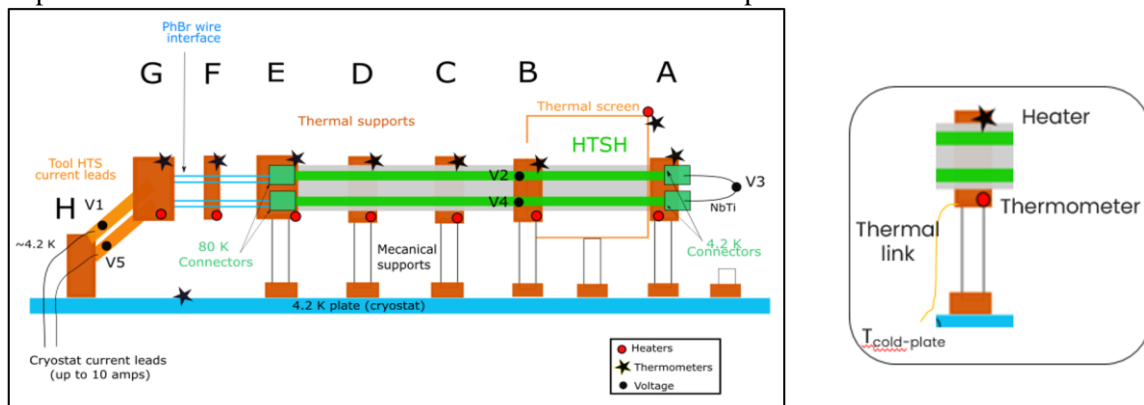


Figure 4. Scheme of the thermal characterization setup and details of a separate interface.

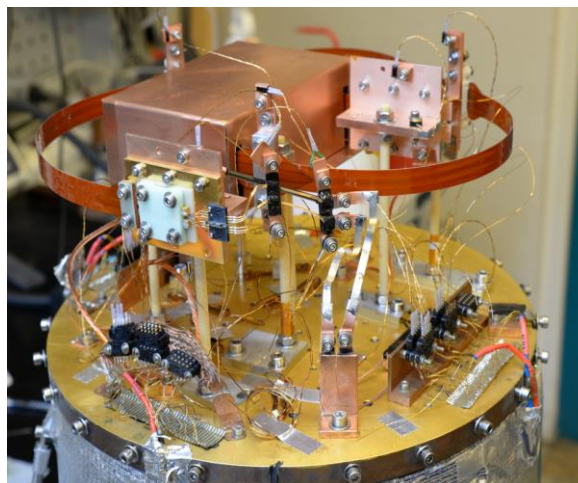


Figure 5. Test setup

The assembly of the test setup including the harness is presented in figure 5. As a first step, it has been calibrated without the HTS Harness and then used with the HTS Harness. The thermal links have been adapted as a compromise between a moderate power use (and dissipated on the helium bath of the cryostat) and precise accuracy.

3.2. Experimental characterization plan

The main properties to validate are the heat loads on the 4 K interface in standard operation. These measurements have been separated in three sub-measurements:

- Measurements of heat conductivity from 30 K to 4 K
- Validation of the low impact of 80 K temperature stage on the conduction to the 4 K interface (efficiency of the 30 K heat sinking on the support)
- Validation of joule losses dissipation at 4 K
- Estimation of the radiation on the 4 K interface from a 30 K environment

Other measurements include:

- Evaluation of the power on the 30 K interface from the measurements with $T_w = 80$ K
- Validation of operation with an 80 K and 85 K warm interface
- Validation of operation with additional heat load at the 80 K / 85 K interface

3.3. Experimental measurements of 4 K heat loads

The measurement of the conductive heat load is done by measuring the variation of power on post A while the post B temperature varies from 4 K to 40 K, with a nominal value at 30 K. During these measurements, the screen temperature was kept at 30 K. The results are presented and compared with the conduction calculation on Figure 6. The calculation is based on the heat conductivity of figure 1 and the good agreement between these two sets of data demonstrates in a way the setup accuracy.

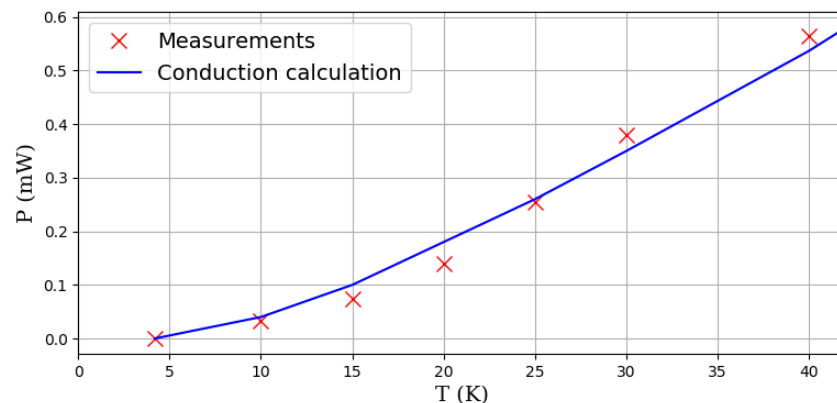


Figure 6. Thermal conductivity contribution to heat load on 4 K stage

The radiation is measured by the contribution of the effect of the shield temperature. It is difficult to predict because of the uncertainty on the emissivity value of the harness as well as its real form factor. It will also be difficult to extrapolate to future instrument, but gives an order of magnitude that could be reduced with proper integration. The support C is regulated at 30 K while the screen temperature is raised from 4 K to 40 K. The results are presented in figure 7 and the power is again the variation of power measured on post A. To compare to radiation, a power law of 4, adjusted to fit the 30 K data is presented on the chart. Surprisingly, the data do not follow precisely a power 4 plot, which could be explained by a variation of emissivity or by other difficulties due to radiation in the cryostat.

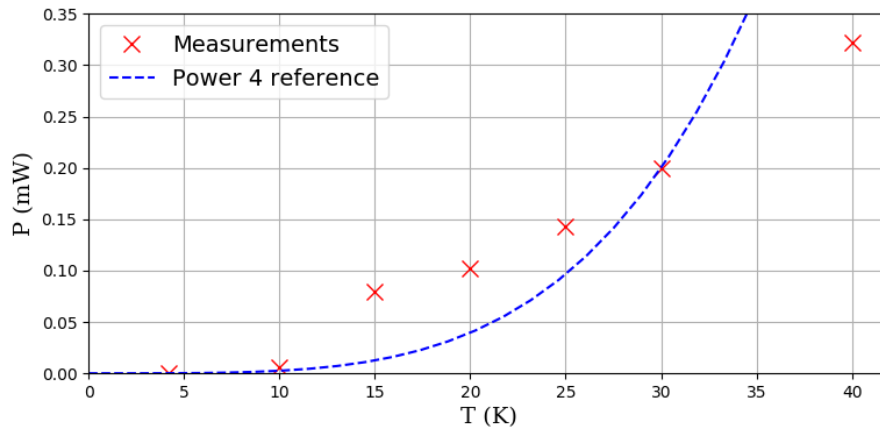


Figure 7. Radiation contribution to heat load on 4 K stage

The Joule losses contribution could not be representatively measured in the initial setup because of an inadequate design, which prevented us from applying the desired torque on electrical joints at 4 K. Instead, a separated and dedicated measurement has been done as presented on Figure 8. It includes two M3 screws and a copper plated surface representative of our design. The torque on the two screws is changed, the setup then immersed in liquid helium and the resistance measured electrically, which could then be translated in Joule losses evaluation. More detailed studies on contact resistances are found in the literature such as [7]. For a resistance of $2 \mu\Omega$, the joule losses at 2 A would be $8 \mu\text{W}$ per contact or $16 \mu\text{W}$ total. This value can easily be achieved with a 0.5 N.m torque compatible with M3 screws.

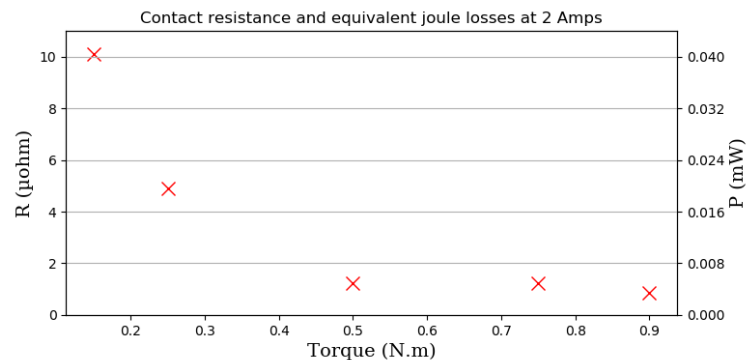


Figure 8. Setup and Joule losses evaluation

Based on these measurements, the contribution of heat load from the 30 K interface to the 4 K level is summarized in Table 2.

Table 2. Contribution at 4 K

Contribution	Value
Conductive 30 K – 4 K, 250 mm	0.38 mW
Radiation from a 30 K environment	0.20 mW
Joule losses at 2 A operation with torque >0.5 N.m	0.016 mW
Total	<0.6 mW

The total heat load is 0.6 mW, well below our requirement of 1 mW. It is, however, probably too large for a design with multiple ADR stages. This heat load is dominated by the heat conduction of the

REBCO tape with Ag cap layer, which, as shown in figure 1, could be reduced by a factor of 4 using an AgAu stabilizing layer. The second contribution is the radiation which depends largely on the final setup and would be severely minimized if either a lower than 30 K environment would be used or a reflective layer would be deposited on the Kapton laminate.

3.4. Additional measurements

The conductivity on the 30 K interface has been measured as well using similar heat flow method. A targeted goal below 30 mW was devised by ESA and a calculation based on thermal conductance predicted a conductive heat load of 2 mW. Measurements have confirmed this calculation with values of 1.2 mW.

Operation at 80 K and 85 K interface has been demonstrated. The performance was limited when applying a heat load of 600 mW on the 80 K interface. This differs from measurements on the first model demonstrating a lack of reproducibility of the thermal interface. This is explained by the difficulty in reproducing the thermal contact on the 80 K interface with low torque. A simpler design, with only one thermal interface instead of two in the current design has been proposed following this demonstration.

Additional mechanical validations have been performed prior to these characterizations including 1000 cycles bending on a radius of 50 mm with no measurable degradation.

4. Qualifications

Qualification required by ESA included a thermal cycling sequence, mechanical environment tests and overvoltage validations. To validate these steps, health tests were performed before and after each stage of the campaign.

Thermal cycling was done twenty times in a dedicated setup in the 80 – 300 K range by immersion in a liquid nitrogen bath (see figure 9). In addition, multiple cool downs to 4 K have been performed during the manufacturing process and initial testing phase at KIT and during the testing and characterization at CEA. No degradation has been observed which reinforces our confidence in the robustness of our design.

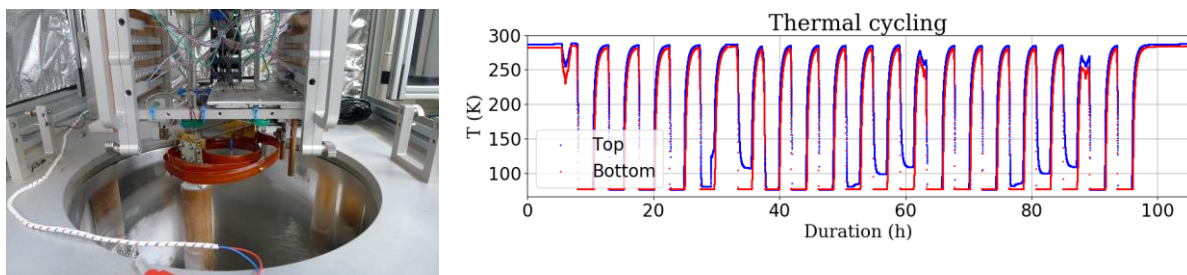
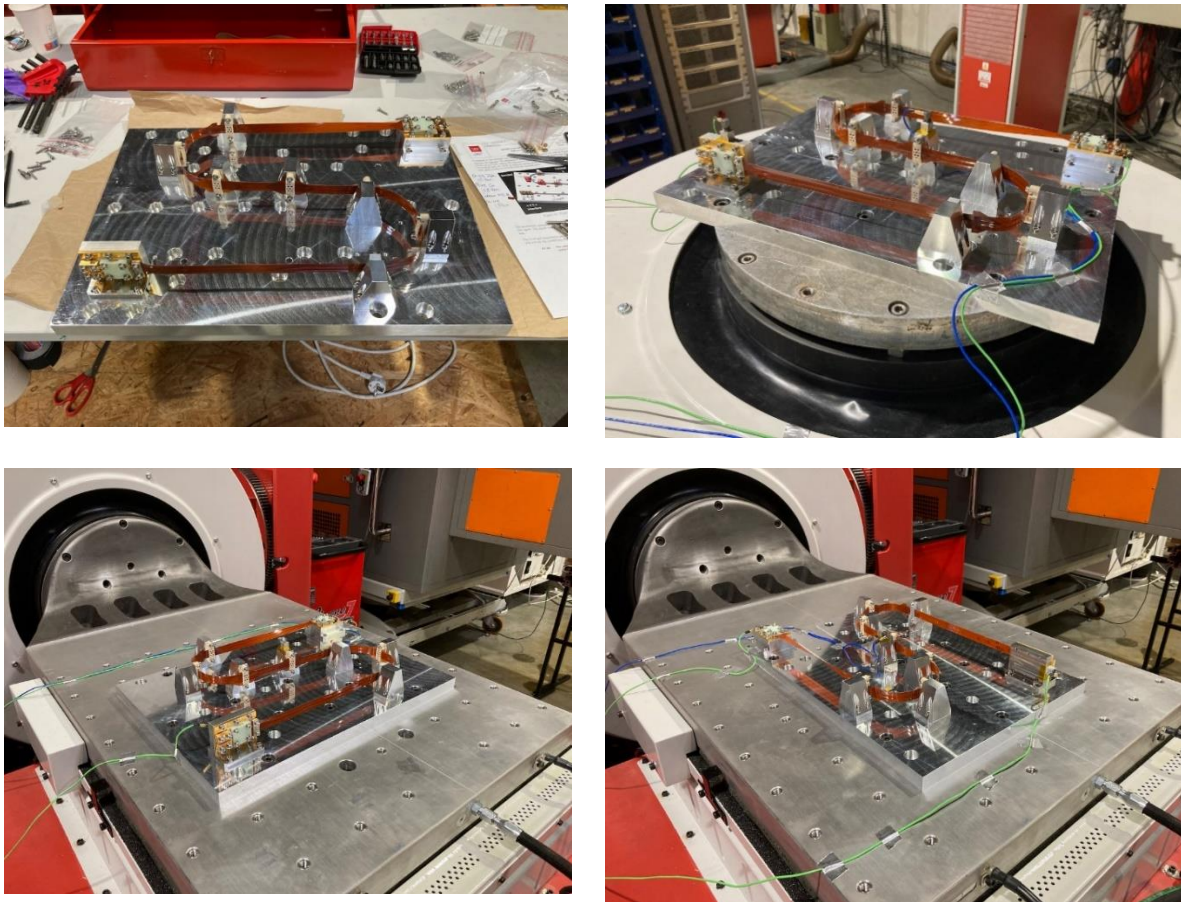


Figure 9. Thermal cycling setup and temperature measurements on top and bottom of the setup

Mechanical qualifications were done on a dedicated vibration testing-table (Figure 10) and qualification up to 13 G RMS (random) has been made. In addition, shock tests (up to 2000 g) were performed with no visible degradation or evolution of the low frequency signature.

Table 3. Summary of the mechanical requirements

Sine	Random	Shock
5-25 Hz up to 10 mm	20 – 100 Hz: +3 DB/oct	10 Hz : 20 h
25 – 100 Hz : 25 g	100 -300 Hz: 0.3 g ² /Hz	1 000 Hz : 2 000 g
Sweep rate : 2 oct/min	300-2 000 Hz : - 5 DB/Oct	10 000 Hz : 2000 g
	Global 13.1 g RMS	
	Duration 2 min/axis	

**Figure 10.** Harness on dedicated vibration testing table (vertical as well as horizontal axes)

Following the full campaign, additional health tests were performed. These standard health test measurements are done with the harness immersed in liquid nitrogen, using currents up to 20 A and measuring the overall voltage. The measurements are presented in Figure 11 and are all below 10 μ V, in the range of our measurement setup sensibility and parasitic offset. No dramatic voltage increase, even up to 20 A, has been observed demonstrating that the integrity of the harness has been kept.

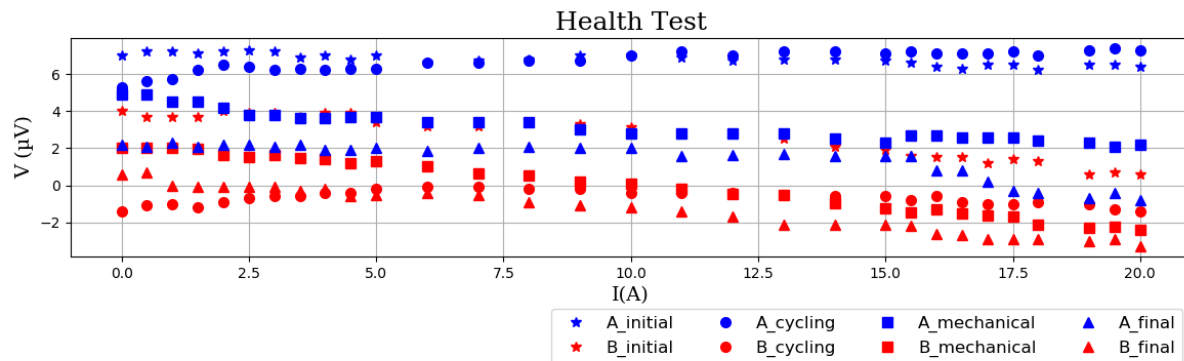


Figure 11. Health tests

5. Perspectives and conclusions

Throughout this activity, a full harness assembly, utilizing state-of-the-art HTS REBCO tapes, has been designed and two engineering models have been manufactured and tested. The necessary manufacturing processes have been established and improved to provide a reliable and repeatable design and product.

The comprehensive testing and qualifications activities have demonstrated that the desired specifications are achieved. Improvements are proposed such as the use of AgAu coated tape and simplified thermal interfaces. The interface at 4 K were tested independently and it has been demonstrated that the use of two M3 screws with 0.5 N·m torque would limit the joule losses at 4 K to a negligible value.

6. Reference

- [1] Barret, D. et al. « The Athena X-ray Integral Field Unit: a consolidated design for the system requirement review of the preliminary definition phase ». *Experimental Astronomy*, 2023, 1–54.
- [2] Chassaing, C., et al. « 15K Pulse Tube Cooler for Space Missions ». In *Cryocoolers*, 18:27-32, 2014.
- [3] Sato, T. et al., « Development status of the mechanical cryocoolers for the Soft X-ray Spectrometer on board Astro-H ». *Cryogenics*, 2014. <https://doi.org/10.1016/j.cryogenics.2014.04.022>.
- [4] Schlachter, S. I. et al, Properties of MgB₂ superconductors with regard to space applications; *Cryogenics* 46 (2006) 201–207.
- [5] Canavan, E. R., B. L. James, T. P. Hait, A. Oliver, et D. F. Sullivan. « The Astro-H High Temperature Superconductor Lead Assemblies ». *Cryogenics*, 2014. <https://doi.org/10.1016/j.cryogenics.2014.06.003>.
- [6] Schlachter, S. I., et al. « Development and Test of High-Temperature Superconductor Harness for Cryogenic Instruments on Satellites ». *IEEE Transactions on Applied Superconductivity* 33, n° 5 (2023): 1–5.
- [7] Blondelle, F., A. Sultan, E. Collin, et H. Godfrin. « Electrical Conductance of Bolted Copper Joints for Cryogenic Applications ». *Journal of Low Temperature Physics* 175, n° 5-6 (7 mars 2014): 877-87. <https://doi.org/10.1007/s10909-014-1142-4>.

Acknowledgments

This work is partially funded by ESA under grant 4000133578/20/NL/FE. We wish to thank Laurent Clerc for the experimental work and his expertise in the set up and experimental measurements, Diane Dherbecourt for her involvement and discussion in the project and Alissia Weyer for her participation in the initial setup calibration. Thanks to Florian Bancel for the design of the experimental setup.